Nonlinear inverse bremsstrahlung in solid-density plasmas

S. Kato, R. Kawakami,* and K. Mima
Institute of Laser Engineering, Osaka University, Suita, Osaka 565, Japan
(Received 31 August 1990; revised manuscript received 17 December 1990)

The laser intensity dependence of the inverse bremsstrahlung absorption coefficient in a strongly coupled plasma is investigated, where the electron quiver velocity ($v_0=eE_0/m\omega_0$) and excursion length ($r_0=eE_0/m\omega_0^2$) in the laser electric field are finite in comparison with the electron thermal velocity and shielding distance, respectively. In plasmas produced by an ultrashort pulse laser, the electron and ion temperatures are not in thermal equilibrium, and the electron temperature is higher than the ion temperature. Since ions are strongly coupled in such plasmas, the ion-ion correlation is described by the hypernetted-chain equation. On the other hand, the electron-ion correlation is described by linear-response theory. By using those correlation functions, the high-frequency conductivity and the laser absorption coefficients are evaluated. The results are applied to a recent experiment on reflectivity [Phys. Rev. Lett. **61**, 2364 (1988)]. The analysis discloses the laser intensity dependence of the ultrashort-pulse-laser absorption rate.

I. INTRODUCTION

Recently, plasmas produced by an intense ultrashort-pulse (pulse width less than 1 ps) laser has attracted much interest.[1-3] Ultrashort-pulse lasers heat a solid target before any expansion occurs. In such a case, the plasma scale length is less than the laser skin depth. Consequently, the ultrashort-pulse-laser radiation directly interacts with a solid-density plasma.

Under the irradiation of a high-intensity subpicosecond-pulse laser, the electron heating time is less than or comparable to that for electron-ion energy relaxation. Namely, the ion temperature is lower than the electron temperature, and ions are coupled strongly. We define the ion-ion and electron-ion Coulomb coupling constants Γ_{ii} and Γ_{ie} by

$$\Gamma_{ii}=Z^2e^2/k_BT_ia_i \ , \tag{1}$$

$$\Gamma_{ie}=Ze^2/k_BT_ea_i \ , \tag{2}$$

where a_i is the average ion radius $(\frac{3}{4}\pi n_i)^{1/3}$, and n_i, Ze, T_i, and T_e are the ion number density, effective ion charge, and temperatures of ion and electron, respectively. The ion-ion correlation function is described by the hypernetted-chain (HNC) equation, which is known as a good approximation when $10\geq\Gamma_{ii}\geq 1$.[4,5] However, the electron-ion and electron-electron couplings may be weak, and the electron-ion correlation is described by the linear-response theory.

The absorption coefficients in a solid-density plasma have been given by several authors.[5-11] However, the effects of finite electron-excursion length have not been treated exactly except for the work of Jones and Lee[9] and Rae and Burnett.[10] In this paper, we derive a basic equation for the electron distribution function in order to take into account effects of the finite electron-excursion length on the laser absorption. The laser intensity dependence of the nonlinear absorption has been given by Rae and Burnett. However, their result is valid only for weakly coupled and nondegenerate plasmas. Furthermore, we analyze the recent experimental results of reflectivity in such a plasma by using our absorption rate.

II. THEORETICAL MODEL AND DERIVATION OF BASIC EQUATION

We derive a basic equation for the electron distribution function in the presence of an intense laser field. Since we are interested in the laser absorption, only electron-ion collision is taken into account. The formulation which we use in this section is analogous to that of Jones and Lee.[9]

The laser electric field is assumed to be given by

$$\mathbf{E}(t)=\mathbf{E}_0\cos(\omega_0t) \ , \tag{3}$$

where ω_0 is the laser frequency. In the absence of collisions, the electron orbit in the laser field is given by

$$\mathbf{v}=\mathbf{v}'+\mathbf{v}_0\sin(\omega_0t) \ , \tag{4}$$

$$\mathbf{r}=\mathbf{r}'+\mathbf{r}_0\cos(\omega_0t) \ , \tag{5}$$

where $\mathbf{r}'$ and $\mathbf{v}'$ are the initial electron position and velocity, and $\mathbf{v}_0$ and $\mathbf{r}_0$ are given by

$$\mathbf{v}_0=-e\mathbf{E}_0/m\omega_0, \quad \mathbf{r}_0=e\mathbf{E}_0/m\omega_0^2 \ , \tag{6}$$

respectively. When we get on a frame which oscillates with velocity $\mathbf{v}_0\sin(\omega_0t)$, the electron orbits are straight lines, and the ions oscillate with frequency ω_0 instead. An electron-ion collision, in this frame, can be regarded as a collision between an electron and a harmonic oscillator of frequency ω_0.

The temporal evolution of the electron distribution function in the oscillating frame is described by the Pauli equation, in which transition probability is evaluated by the Born approximation, as discussed later.

The charge distribution of ions is given by

$$\rho(\mathbf{r},t)=\sum_{j=1}^{N_i} Ze\delta(\mathbf{r}-\mathbf{r}_j+\mathbf{r}_0\cos\omega_0 t) , \tag{7}$$

where N_i is the number of ions. The Fourier transform of Eq. (7) yields

$$\rho(\mathbf{k},\omega)=\sum_{j=1}^{N_i}\sum_{n=-\infty}^{\infty} Ze2\pi\delta(\omega+n\omega_0)i^n\mathbf{J}_n(\mathbf{k}\cdot\mathbf{r}_0)e^{-i\mathbf{k}\cdot\mathbf{r}_j} , \tag{8}$$

where $J_n(x)$ is a Bessel function of the first kind.

Since the electron-ion Coulomb coupling constant $\Gamma_{ei}\leq 1$, the electron shielding of the ion Coulomb field is evaluated by the linear-response theory. The electrostatic potential at a position $\mathbf{r}$ is then given by

$$\Phi(\mathbf{r},t)=-\int\frac{d\mathbf{k}}{(2\pi)^3}\frac{d\omega}{2\pi}\frac{4\pi e}{k^2}\frac{1}{\epsilon(\mathbf{k},\omega)}\rho(\mathbf{k},\omega) \times\exp[i(\mathbf{k}\cdot\mathbf{r}-\omega t)] , \tag{9}$$

where $\epsilon(\mathbf{k},\omega)$ is the dielectric-response function. Substituting Eq. (8) into Eq. (9) and using an electron trajectory given by

$$\mathbf{r}(t)=\mathbf{r}'+\mathbf{v}'t , \tag{10}$$

we have

$$\Phi(\mathbf{r}(t),t)=-\int\frac{d\mathbf{k}}{(2\pi)^3}\sum_{j=1}^{N_j}\sum_{n=-\infty}^{\infty}\frac{4\pi Ze^2}{k^2}\frac{1}{\epsilon(\mathbf{k},-n\omega_0)}i^nJ_n(\mathbf{k}\cdot\mathbf{r}_0)\exp(-i\mathbf{k}\cdot\mathbf{r}_j+in\omega_0 t)\exp[i\mathbf{k}\cdot(\mathbf{r}'+\mathbf{v}'t)] . \tag{11}$$

The wave-number spectrum of potential fluctuations averaged over a laser period is written as

$$\langle|\Phi(\mathbf{k})|^2\rangle=\sum_{n=-\infty}^{\infty}\left|\frac{4\pi Ze^2}{k^2}\right|^2\frac{1}{|\epsilon(\mathbf{k},-n\omega_0)|^2}\mathbf{J}_n^2(\mathbf{k}\cdot\mathbf{r}_0)N_iS(\mathbf{k}) , \tag{12}$$

where $S(\mathbf{k})$ is the structure factor of the ion, which is defined by

$$S(\mathbf{k})=\frac{1}{N_i}\left\langle\sum_{i,j=1}^{N_i}\exp[i\mathbf{k}\cdot(\mathbf{r}_i-\mathbf{r}_j)]\right\rangle , \tag{13}$$

and $\langle\ \rangle$ is the ensemble average over ion configurations.

The kinetic equation for the electron distribution function in a laser field is given as follows when Eq. (12) and the Born approximation are used:

$$\frac{\partial f(\mathbf{p})}{\partial t}=\frac{4Z^2e^4}{\hbar}n_i\sum_{n=-\infty}^{\infty}\int d\mathbf{k}\frac{1}{k^4}\frac{1}{|\epsilon(\mathbf{k},-n\omega_0)|^2}J_n^2(\mathbf{k}\cdot\mathbf{r}_0)S(\mathbf{k})\delta(E_{\mathbf{p}+\hbar\mathbf{k}}-E_{\mathbf{p}}-n\hbar\omega_0)[f(\mathbf{p}+\hbar\mathbf{k})-f(\mathbf{p})] , \tag{14}$$

where $\mathbf{p}$ is the electron momentum. This equation is nothing but the Pauli equation. Using this equation, we evaluate the absorption rate of a high-intensity laser in solid density plasmas.

III. NONLINEAR INVERSE BREMSSTRAHLUNG

The electron heating rate by laser absorption is evaluated by

$$\frac{\partial U_k}{\partial t}=\int\frac{\partial f(\mathbf{p})}{\partial t}\frac{p^2}{2m}\frac{2d\mathbf{p}}{(2\pi\hbar)^3} . \tag{15}$$

We assume that the electron distribution function in the right-hand side of Eq. (15) can be approximated by the Fermi-Dirac distribution function

$$f(\mathbf{p})=\left[1+\exp\left[\frac{(p^2/2m)-\mu}{k_BT_e}\right]\right]^{-1} , \tag{16}$$

where μ is the chemical potential, to obtain from Eqs. (14) and (15)

$$\frac{\partial U_k}{\partial t}=\frac{4Z^2e^4m^2\omega_0}{\pi\hbar^4}n_ik_BT_e\sum_{n=1}^{\infty}n\int_0^{\infty}dk\frac{1}{k^3}\frac{1}{|\epsilon(k,n\omega_0)|^2}S(k)F_n(k,\omega_0)B_n(kr_0) . \tag{17}$$

Here

$$B_n(kr_0)=\int_{-1}^{1}dx\,\mathbf{J}_n^2(kr_0x) , \tag{18}$$

$$F_n(k,\omega_0)=\ln\left[\frac{1+\exp\left[\frac{\mu}{k_BT_e}-\frac{\hbar^2}{2mk_BT_e}\left[\frac{nm\omega_0}{\hbar k}-\frac{k}{2}\right]^2\right]}{1+\exp\left[\frac{\mu}{k_BT_e}-\frac{\hbar^2}{2mk_BT_e}\left[\frac{nm\omega_0}{\hbar k}+\frac{k}{2}\right]^2\right]}\right] . \tag{19}$$

The total electromagnetic energy U is given by

$$U=\frac{1}{8\pi}\left[\frac{d(\omega_0\epsilon)}{d\omega_0}\overline{E^2}+\overline{B^2}\right] , \tag{20}$$

where E and B are the electromagnetic field, ϵ is the dielectric-response function, and the bar denotes an average with respect to time. For $\omega_0>\omega_p$,

$$\overline{B^2}=[1-(\omega_p/\omega_0)^2]\overline{E^2} , \tag{21a}$$

and for $\omega_0<\omega_p$,

$$\overline{B^2}=[(\omega_p/\omega_0)^2-1]\overline{E^2} . \tag{21b}$$

In the limit of small collision frequency,

$$\frac{d(\omega_0\epsilon)}{d\omega_0}=1+\left[\frac{\omega_p}{\omega_0}\right]^2 . \tag{22}$$

The total electromagnetic energy is then given by

$$U=\begin{cases}\overline{E^2}/4\pi & \text{for } \omega_0>\omega_p \quad (23a)\\ \overline{E^2}/4\pi(\omega_p/\omega_0)^2 & \text{for } \omega_0<\omega_p \quad (23b)\end{cases} .$$

Dividing Eq. (17) by U of Eqs. (23a) and (23b), we obtain the absorption rate (in s^{-1}) as follows:

$$A=\frac{32Z^2e^6}{\hbar^4\omega_0^3}K\frac{1}{r_0^2}n_ik_BT_e\sum_{n=1}^{\infty}n\int_0^{\infty}dk\frac{1}{k^3}\frac{1}{|\epsilon(k,n\omega_0)|^2}S(k)F_n(k,\omega_0)B_n(kr_0) , \tag{24}$$

and

$$K=\begin{cases}1 & \text{for } \omega_0>\omega_p \quad (25a)\\ (\omega_0/\omega_p)^2 & \text{for } \omega_0<\omega_p , \quad (25b)\end{cases}$$

where ω_p is the plasma frequency, and r_0 is the electron-excursion length.

Note that this formula for the absorption rate depends upon the electron-excursion length, namely, the laser intensity.

For $\omega_0>\omega_p$, we divide Eq. (18) by the group velocity v_g to obtain the absorption coefficient of laser light per unit length (in cm^{-1}):

$$\eta=\frac{32Z^2e^6}{c\hbar^4\omega_0^2(\omega_0^2-\omega_p^2)^{1/2}}\frac{1}{r_0^2}n_ik_BT_e\sum_{n=1}^{\infty}n\int_0^{\infty}dk\frac{1}{k^3}\frac{1}{|\epsilon(k,n\omega_0)|^2}S(k)F_n(k,\omega_0)B_n(kr_0) . \tag{26}$$

In the limit of small electron-excursion length,

$$B_n(kr_0)=\tfrac{1}{6}(kr_0)^2 , \tag{27}$$

Eq. (26) is reduced to the Kawakami's expression[5] when we set by $\epsilon(k,n\omega_0)=1$. In the classical limit ($\hbar\to0$), this absorption rate agrees with the expression given by Dawson and Oberman.[6]

IV. NUMERICAL CALCULATION

When ion-ion coupling is not weak, the Debye-Hückel model is no longer applicable to evaluate $S(k)$ of Eq. (24). The ion correlations in high-density plasmas are described by some integral equations. Since we are interested in the parameter region of $1\le\Gamma_{ii}\le10$, we may employ the hypernetted-chain equation, which is known to work as a good approximation when the ion-ion coupling pa-

rameter is not so large.[4,5] We solve the hypernetted-chain equation to obtain $S(k)$. The HNC equation is given by

$$1+h(r)=\exp\left[-\frac{\Phi_{ii}(r)}{k_B T_i}+h(r)-c(r)\right], \tag{28}$$

supplemented by the Ornstein-Zernike relation

$$h(r)=c(r)+n_i\int c(|\mathbf{r}'-\mathbf{r}|)h(r')d\mathbf{r}', \tag{29}$$

where $c(r)$ is the direct correlation function. The radial distribution function of the ion $g(r)$ and the structure factor $S(k)$ are related to $h(r)$ as

$$g(r)=1+h(r) \tag{30}$$

$$S(k)=1+n_k\int h(r)e^{i\mathbf{k}\cdot\mathbf{r}}d\mathbf{r}. \tag{31}$$

In the HNC equation, we use the ion Coulomb potential Z^2e^2/r without electron shielding. The structure factor $S(k)$ is given by the HNC equation.

The electron-ion and electron-electron couplings may be weak, and the electron-ion correlation is described by the linear-response theory. The dielectric-response function included with the electron degeneracy and local-field correction is given by the Ichimaru *et al.*[12] When the local-field correction is ignored, the dielectric response of the electron degeneracy and collisionless plasmas are given by[13]

$$\epsilon(k,\omega)=1-\frac{4\pi e^2}{k^2\hbar}\int\frac{f(\mathbf{p}+\hbar\mathbf{k})-f(\mathbf{p})}{\mathbf{k}\cdot\mathbf{p}/m-\omega+\frac{\hbar k^2}{2m}-i\eta}\frac{2d\mathbf{p}}{(2\pi\hbar)^3}, \tag{32}$$

where η is the positive infinitesimal. When the collision frequency is larger than the plasma frequency, this dielectric-response function of the collisionless plasmas may not be valid. This problem is discussed in the last part of this section. We carry out the integration of Eq. (24) numerically by using the expressions of Eqs. (31) and (32) to obtain the absorption rate A.

The electromagnetic field amplitude is simply related to the laser intensity in the vacuum by $I(W/\mathrm{cm}^2)=(c/8\pi)\overline{E^2}(10^{-7})$, where E is in units of statvolt/cm. However, in the plasma, the relation between the laser intensity and the electromagnetic field depends on the plasma density. Therefore, we use $k_D r_0$ or v_0/v_e instead of the laser intensity, where k_D and v_e are the Debye wave number and the electron thermal velocity, respectively.

The summation in Eq. (24) is taken up to $n=n_{\max}$, where $n_{\max}$ is chosen so as to keep the truncation error smaller than 10^{-3}. However, when $v_0/v_e>10$, a convergence of the summation is not good, and we truncated the summation at $n=350$. In such a case, the numerical results of the absorption rate may be lower by about 20% than the true values.

For examples, the absorption rate A of Eq. (24) is evaluated for $T_e=600$ eV, $T_i=200$ eV, $Z=10$, λ (laser wavelength) $=0.53$ μm. For electron densities $n_e=10^{21}$ cm^{-3} (for an underdense plasma) [case 1(a)] and $n_e=10^{24}$ cm^{-3} (for a solid density plasma) [case 1(b)], the numerical results are shown in Figs. 1(a) and 1(b), respectively. Figures 1(a) and 1(b) show that the absorption rate decreases when $k_D r_0$ increases and is greater than unity. The critical values of $k_D r_0$ where the absorption rate begins to decrease are different between the cases 1(a) and 1(b). Namely, A is reduced by the nonlinearities for $k_D r_0>0.5$ in Fig. 1(a) and for $k_D r_0>16$ in Fig. 1(b). In order to explain this difference, we look at the dependence of the absorption rate on the ratio of the quiver velocity to the thermal velocity,

$$v_0/v_e=(\omega_0/\omega_p)k_D r_0. \tag{33}$$

For cases 1(a) and 1(b), $\omega_p/\omega_0\approx 0.5$ and 16, respectively. Therefore, the critical values of v_0/v_e are approximately 1.0 for both cases. We can say that the nonlinear effect reduces the absorption rate significantly when $v_0/v_e\gtrsim 1$. On the other hand, we show the density dependence of the nonlinear reduction of absorption rate in Fig. 2. We introduced the ratio of the nonlinear absorption rate to

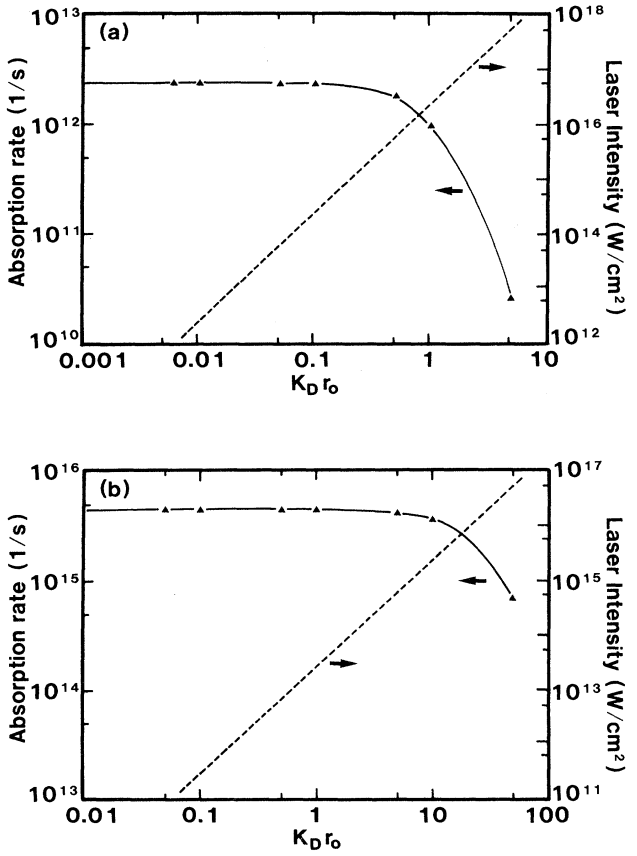

FIG. 1. (a) Absorption rate for case 1(a). The dashed line is the laser intensity that is given by the relation in vacuum $[I(\mathrm{W/cm}^2)=(c/8\pi)\overline{E^2}10^{-7}]$ as a function of the electric field. (b) Same as (a) for case 1(b).

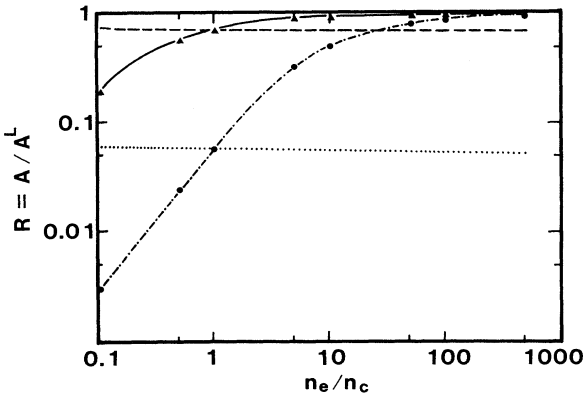

FIG. 2. Ratio R for $T_e=600$ eV, $T_i=200$ eV, $Z=10$, $\lambda=0.53$ μm. The solid, dashed-dotted, dashed, and dotted lines are the ratios where $k_D r_0=1$, $k_D r_0=5$ $v_0/v_e=1$, and $v_0/v_e=5$ are fixed, respectively.

the linear one,

$$R=\frac{A}{A^L}\ , \tag{34}$$

where A^L is the absorption rate in the limit of low laser intensity. Actually, A^L is obtained by using Eq. (27). Figure 2 shows R as a function of the electron density for various $k_D r_0$ and v_0/v_e. Other parameters are the same as for Figs. 1(a) and 1(b). The ratios are almost the same for the electron density from $n_e/n_c=0.5-500$, when v_0/v_e is fixed where n_c is the cutoff density. Figure 3 shows R as a function of the v_0/v_e for $T_e=600$ eV, $T_i=200$ eV, $Z=10$, $\lambda=0.53$ μm. When $v_0/v_e=1$, the absorption rate decreases by approximately 30%. Note here that all of the above discussions on the density dependences of the nonlinear absorption are restricted to the case when the electrons are not degenerate. The absorption rate varies with the density even for a fixed v_0/v_e when plasmas are degenerate, as shown in the following.

Shown in Fig. 4(a) is the linear absorption rate Eq. (24) in the low laser intensity limit as a function of the electron temperature for $Z=10$, $\lambda=0.53$ μm, $n_e=10^{24}$ cm^{-3}. Figure 4(a) indicates that the absorption rate A is proportional to the $\frac{-3}{2}$ power of the electron temperature ($T_e^{-3/2}$) in the high-temperature limit, namely in the weak-coupling limit. When T_e is lower than the Fermi temperature (T_F), Fig. 4(a) shows that A increases when the electron temperature increases until it reaches Fermi temperature (T_F). Note that in Fig. 4(a), $T_F=36$ eV. In order to see how the nonlinearity depends upon the electron temperature, we show Fig. 4(b). Figure 4(b) shows R as a function of the electron temperature for $v_0/v_e=1.0$ and 5.0. In the high-temperature limit ($T_e>T_F$), the ratio R is almost the same for the same $v_0/v_e=5.0$. Note

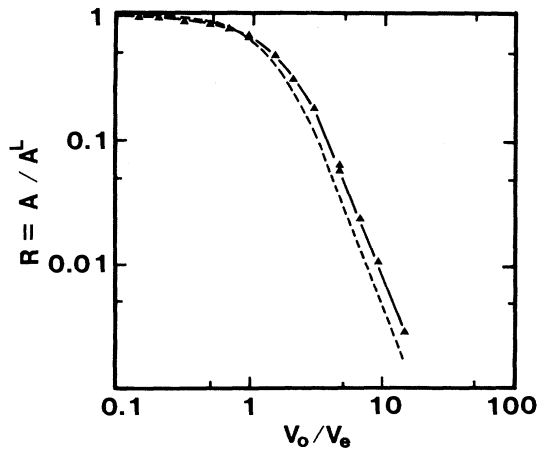

FIG. 3. Ratio R for the v_0/v_e for $T_e=600$ eV, $T_i=200$ eV, $Z=10$, $\lambda=0.53$ μm.

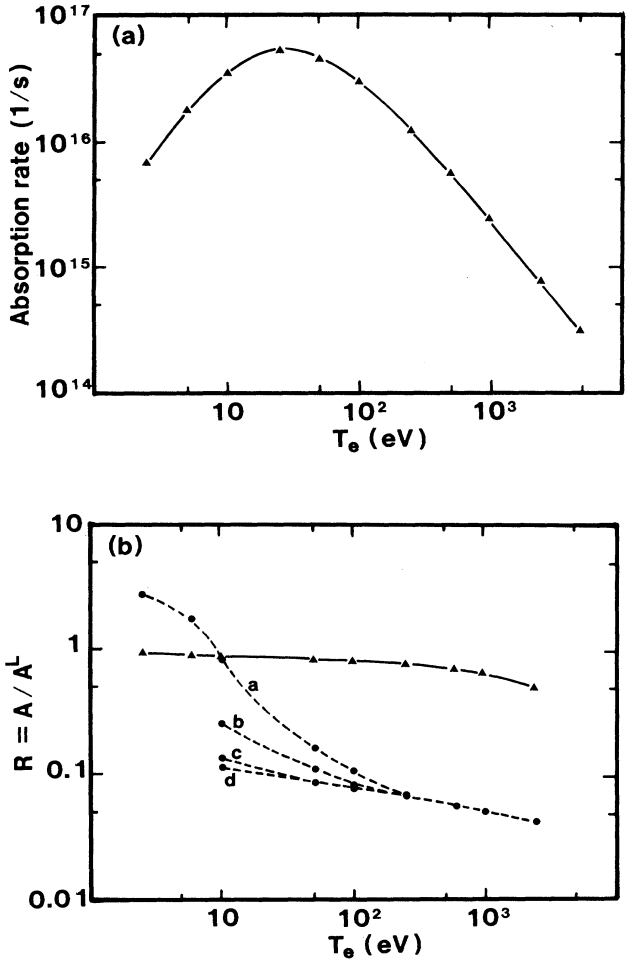

FIG. 4. (a) Absorption rate Eq. (24) as a function of the electron temperature for $Z=10$, $\lambda=0.53$ μm, $n_e=10^{24}$ cm^{-3}, $v_0/v_e=10^{-4}$. (b) Ratio R for $T_i=T_e/3$, $Z=10$, $\lambda=0.53$ μm. The solid line is for $n_e=10^{24}$ cm^{-3} and $v_0/v_e=1$. The dashed lines a, b, c, and d are for $v_0/v_e=5$ and $n_e=10^{21}$ 10^{22}, 10^{23}, and 10^{24} cm^{-3}, respectively.

that the dashed and dotted lines overlap each other in the case of $T_e > 200$ eV. However, in the low-temperature regime ($T_e \leq T_F$), where the electrons are degenerate, the ratios are different for the different electron density. The reduction of absorption for $n_e = 10^{24}$ cm^{-3} ($T_e \leq T_F = 36$ eV) is less than that for the low-density case (e.g., $n_e = 10^{21}$ cm^{-3} and $T_F < T_e$). Sometimes the nonlinear absorption rate is even higher than the linear one, since the removal of the degeneracy occurs by the quiver motion. Figure 4(b) also indicates that the ratios decrease for a fixed v_0/v_e when the electron temperature increases. For $v_0/v_e = 1$, the absorption rate decreases by ~ 20–$35\,\%$ for the electron temperature from 100 to 1000 eV. These results suggest that we can take into account the nonlinear effects by replacing v_e by $(v_0^2/3 + v_e^2)^{1/2}$ in the formula of the linear absorption rate. Namely, the absorption rate is reduced by $R = 1/(1 + v_0^2/3v_e^2)^{3/2}$, which is shown in Fig. 3 by a broken line.

Note that in the Born approximation, both the initial and final states of the electron are assumed to be the plane wave.[11] When ionization or recombination occurs by the laser absorption or by the emission, the Born approximation breaks down. Namely, the bound-free transition during the laser absorption has to be appropriately taken into account. This will be discussed in a future paper.

In the case of low temperature and not so high density (T_F is not high), the electron-ion collision frequency can be larger than the laser frequency. In that parameter regime, the electric-response function used here may not be valid. Namely, we need to include the electron-ion collision frequency in the dielectric-response function. However, the formula for the absorption rate Eq. (24) may be valid even in that case if $\epsilon(k,\omega)$ is appropriately given.

V. COMPARISON WITH EXPERIMENTAL RESULTS

We assume a sharp vacuum-solid boundary because the plasma surface does not expand much in a ultrashort pulse laser. In other words, we assume that the plasma scale length is much less than the laser skin depth.

In this case, the reflectivities for s-polarized and p-polarized laser light are given by

$$R = \left| \frac{k - \kappa}{k + \kappa} \right|^2 , \tag{35a}$$

and

$$R = \left| \frac{(k-\kappa)\cos\theta - k[1-(1/\epsilon)]\sin^2\theta}{(k+\kappa)\cos\theta + k[1-(1/\epsilon)]\sin^2\theta} \right|^2 , \tag{35b}$$

respectively. Here k and κ are the wave numbers, $k = \omega_0/c$ and $\kappa = \omega_0/c(n^2 - \sin^2\theta)^{1/2}$, in the vacuum and a plasma, respectively, where n is the complex index of refraction and θ is the angle of incidence.

We assumed that the complex index of refraction is given by the Drude model. In this model, the complex index of refraction n is given by $n^2 = 1 + i4\pi\sigma/\omega_0$, where σ is the complex conductivity such that $\sigma = \sigma_r + \sigma_i$, with $\sigma_r = (\nu/4\pi)\xi$ and $\sigma_i = (\omega_0/4\pi)\xi$, with $\xi = \omega_p^2/(\omega_0^2 + \nu^2)$. Here ν is the electron collision frequency, ω_0 is the laser frequency, and ω_p is the plasma frequency ($\omega_p^2 = 4\pi n_e e^2/m$). In high-density plasma ($n_e > n_c$, n_c is the cutoff density), the electron collision frequency is determined consistently with our expression of the laser damping rate (laser absorption rate). When the electron temperature, the ion temperature, the effective ion charge, and the number density of the electron are given, A is estimated by Eq. (24) and the electron collision frequency is given by $\nu = A$ for $\omega_0 < \omega_p$.[6]

We compare our theoretical results [Eqs. (35a) and (35b) with Eq. (24)] with the recent experimental results of the ultrashort-pulse-laser plasma interaction.[1] In the

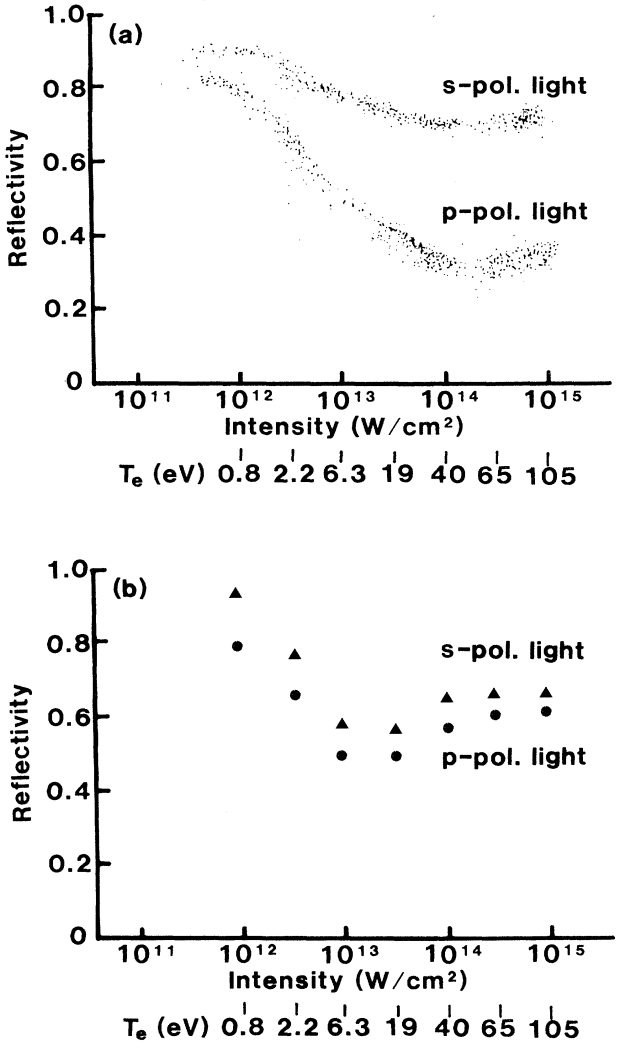

FIG. 5. (a) The experimental results (Ref. 1) showing the reflectivity as a function of laser intensity. (b) The calculation results showing the reflectivity as a function of the laser intensity.

experiment, the laser wavelength is 0.308 μm, the angle of incidence is 45°, the electron temperature was measured, and the effective ion charge was obtained by assuming local thermal equilibrium (LTE). Actually, we calculated the reflectivity as a function of laser intensity for a solid density aluminum plasma. Here the ion temperatures are assumed to be one third of the measured electron temperatures. The experimental results and our results are shown in Figs. 5(a) and 5(b), respectively. The theoretical results reproduce the experimental results for s-polarized light, in which the reflectivity decreases when the laser intensity increases from 10^{11} to 10^{14} W/cm^2, and it is constant for the laser intensity (10^{14}–10^{15} W/cm^2). Physically, the decrease of the reflectivity in $I \leq 10^{14}$ W/cm^2 is explained by the removal of the degeneracy. Namely, more electrons contribute to absorbing the laser radiation when electrons become nondegenerate by laser heating. In the intensity region $10^{14} \leq I \leq 10^{15}$, the electron temperature increases from 40 to 105 eV, and the aluminum ion charge increases from $Z=3$ to $Z=6$. Although the increase of Z enhances the absorption rate, the increase of the electron temperature and the quiver velocity reduces it. In this intensity regime, these two effects compete with each other and keep the absorption rate constant. However, the present model does not explain the differences of the absorption rate between s- and p-polarized light. It is probably necessary to take into account the resonance[14] and/or the quasiresonance[15] absorption to explaining the laser intensity dependence of the absorption rate on the p-polarized light.

VI. DISCUSSION ON THE VALIDITY OF ASSUMPTIONS OF THE PREVIOUS SECTION

In this section, we discuss the validity of three assumptions which were made in the comparison of theoretical results with experiment. They are the stepwise density profile, uniform temperature, and local thermal equilibrium.

A. Density profile

The laser pulse width is a few hundreds of femtoseconds. Therefore, the density scale length of the expanding surface plasma is less than 0.1 μm, which is shorter than the collisionless skin depth of the laser light. Therefore, the plasma density profile is approximated by a stepwise density profile for evaluating the inverse bremsstrahlung absorption rate, although the resonance absorption is more sensitive to the density scale length at the cutoff surface. This is the reason why the agreement of our absorption rate with the experimental results for p-polarized light is poor.

B. Temperature

We use the electron temperature, which is deduced from the experimentally measured expansion velocity. In the numerical analysis, the plasma temperature was assumed to be uniform over the skin depth. This assumption may be justified when the heat wave penetration depth d_T is longer than the skin depth d_s. The depth d_T is approximately evaluated by

$$d_T \approx \sqrt{t\kappa/n_e k_B} \ . \tag{36}$$

For $T_e \approx 10$ eV, $\kappa \approx 5\times 10^8$ erg/cm sec deg (Ref. 16) and $t \approx 0.5$ ps, $d_T \approx 0.05$ μm, which is the order of the skin depth. Therefore, the temperature distribution can be assumed uniform for $T_e \geq 10$ eV. On the other hand, when $T_e \leq 10$ eV for low intensity irradiation, the temperature may not be uniform. Therefore, the detail results on absorption of the low-intensity laser ($I \leq 10^{13}$ W/cm^2) may depend upon the electron heat conduction process. However, the qualitative result, such as the intensity dependence of the absorption rate, may not change, because the absorption occurs mainly on the target surface, whose temperature is experimentally measured.

C. Atomic process

As for the ionization process, we assumed that the relaxation times of ionization, recombination, excitation, and deexcitation processes are much shorter than the laser pulse length. For a solid density plasma, the electron impact ionization rate is greater than 10^{13} sec^{-1}. Therefore, the relaxation times of ionization processes may be shorter than 100 fs. On the other hand, the electron impact excitation rates are much higher than the ionization rates. Therefore, the short laser pulse effects are not important. Furthermore, in the present plasma parameters, the temperature is not so high and the density is so high as to keep collisional excitation rates much higher than radiative decay rate. Therefore, the nonthermal-equilibrium effects may not be essential in the present analysis.

VII. SUMMARY

We derive a kinetic equation for the electron distribution function in a high-density plasma which is heated by an ultrashort-pulse laser. Taking the energy moment of the kinetic equation, the absorption rate of a high-intensity laser light in the high-density plasma is evaluated. In the calculation, ion-ion correlation and electron shielding are taken into account by the HNC equation and the Lindhard dielectric-response function, respectively. Consequently, the absorption rate decreases in the high-intensity range, namely, $v_0/v_e > 1$. When $v_0/v_e = 1$ and 5, the nonlinear effects reduce the absorption rate to about 20–35 % and less than 10% of the linear absorption rate, respectively.

The experimental results for the ultrashort-pulse-laser interaction with plasmas are qualitatively analyzed by using the Drude model with our formula for the absorption rate. Consequently, we found that the reflectivity in the intensity range of $I \leq 10^{14}$ W/cm^2 decreases due to the reduction of electron degeneracy, and the reflectivity is

constant for $I \approx 10^{14}-10^{15}$ W/cm^2. When $I \approx 10^{14}-10^{15}$ W/cm^2, the effects of the increase of the ionization rate and the electron temperature increase compete, and the absorption rate is kept constant. However, further study is necessary to explain the intensity dependence of the absorption rate of p-polarized light.

ACKNOWLEDGMENTS

We would like to thank Dr. H. Takabe, Dr. A. Nishiguchi, Professor K. Nishihara, and Mr. H. Furukawa at the Institute of Laser Engineering (ILE), Osaka University for many useful discussions.

---

*Present address: Sakaihigasi High School, Sakai, Osaka 590-01, Japan.

[1]H. M. Milchberg, R. R. Freeman, and S. C. Davey, Phys. Rev. Lett. **61**, 2364 (1988).
[2]M. M. Murnane, H. C. Kapteyn, and R. W. Falcone, Phys. Rev. Lett. **62**, 155 (1989).
[3]J. C. Keiffer *et al.*, Phys. Rev. Lett. **62**, 760 (1989).
[4]Kin-Chue Ng, J. Chem. Phys. **61**, 2680 (1974).
[5]R. Kawakami, K. Mima, H. Totsuji, and Y. Yokoyama, Phys. Rev. A **38**, 3618 (1988).
[6]J. Dawson and C. Oberman, Phys. Fluids **5**, 517 (1962); J. Dawson, in *Advance in Plasma Physics,* edited by A. Simon and W. B. Thompson (Wiley, New York, 1969), Vol. 1, p. 1.
[7]S. Skupsky, Phys. Rev. A **36**, 5701 (1987).
[8]A. Brunce Langdon, Phys. Rev. Lett. **44**, 575 (1980).
[9]R. D. Jones and K. Lee, Phys. Fluids **25**, 2307 (1982).
[10]S. C. Rae and K. Burnett, Phys. Fluids B **2**, 1015 (1990).
[11]H. Totsuji, Phys. Rev. A **32**, 3005 (1985).
[12]S. Ichimaru, S. Mitake, S. Tanaka, and X. -Z. Yan, Phys. Rev. A **32**, 1768 (1985).
[13]E. M. Lifshitz and L. P. Pitaevskii, *Physical Kinetics* (Pergamon, New York, 1981), Sec. 40.
[14]J. Albritton and P. Koch, Phys. Fluids **18**, 1136 (1975).
[15]F. Brunel, Phys. Rev. Lett. **59**, 52 (1987).
[16]Y. T. Lee and R. M. More, Phys. Fluids **27**, 1273 (1984).